Molecular Biology of the Cell
Vol. 14, 4581–4591, November 2003

PIKfyve Controls Fluid Phase Endocytosis but Not Recycling/Degradation of Endocytosed Receptors or Sorting of Procathepsin D by Regulating Multivesicular Body Morphogenesis

Ognian C. Ikonomov,* Diego Sbrissa,* Michelangelo Foti,† Jean-Louis Carpentier,† and Assia Shisheva*‡

*Department of Physiology, Wayne State University School of Medicine, Detroit, Michigan 48201; and †Department of Morphology, Faculty of Medicine, 1211 Geneva 4, Switzerland

Submitted April 10, 2003; Revised June 9, 2003; Accepted July 7, 2003
Monitoring Editor: Vivek Malhotra

The mammalian phosphatidylinositol (PtdIns) 5-P/PtdIns 3,5-P_2–producing kinase PIKfyve has been implicated in maintaining endomembrane homeostasis in mammalian cells. To address the role of PIKfyve in trafficking processes, we examined the functioning of the biosynthetic, endocytic, and recycling pathways in stable human embryonic kidney 293 cell lines inducibly expressing the wild-type or kinase-defective dominant-negative form. PIKfyve^{WT} or PIKfyve^{K1831E} expression did not affect the processing and lysosomal targeting of newly synthesized procathepsin D. Likewise the rates of transferrin uptake/recycling or epidermal growth factor receptor degradation were not altered upon expression of either protein. In contrast, PIKfyve^{K1831E} but not PIKfyve^{WT} expression markedly impaired the late uptake of fluid phase marker horseradish peroxidase. Inspection of the organelle morphology by confocal microscopy with specific markers in COS cells transiently expressing PIKfyve^{K1831E} showed the Golgi apparatus, end lysosomes, and the recycling compartment indistinguishable from nontransfected cells, despite the dramatic PIKfyve^{K1831E}-induced endomembrane vacuolation. In contrast, we observed a striking effect on the late endocytic compartment, marked by disruption of the dextran-labeled perinuclear endosomal compartment and formation of dispersed enlarged vesicles. Electron microscopy identified the cytoplasmic vacuoles in the PIKfyve^{K1831E}-expressing human embryonic kidney 293 cells as enlarged multivesicular body-like structures with substantially lower number of internal vesicles and membrane whorls. Together, these data indicate that PIKfyve selectively regulates the sorting and traffic of peripheral endosomes containing lysosomaly directed fluid phase cargo through controlling the morphogenesis and function of multivesicular bodies.

INTRODUCTION

Proteins, lipids, or solutes enter the eukaryotic cell by the endocytic pathway comprised of an elaborate membrane system of endosomal vesicles that are distinguished by characteristic morphology, and protein and lipid composition (reviewed in Mukherjee and Maxfield, 2000; Gruenberg, 2001; Miaczynska and Zerial, 2002; Pfeffer, 2003). Efficient sorting mechanisms within early/sorting endosomes rapidly recycle some molecules back to the plasma membrane, whereas others, including soluble species and down-regulated receptors, are transported to prelysosomal compartments/late endosomes/multivesicular bodies (terms used herein interchangeably) and lysosomes for degradation. The endosomal system also receives and sorts cargo proteins from the biosynthetic pathway (reviewed in Hunziker and Geuze, 1996; Ghosh *et al*., 2003). Thus, newly synthesized lysosomal enzymes are diverted from the secretory pathway through binding to one of the two mannose 6-phosphate-receptor (MPR) types. Sequestered into clathrin-coated vesicles at the *trans*-Golgi network (TGN), the enzymes arrive in the prelysosomal compartment, where they dissociate from MPR and are ultimately delivered to lysosomes. The trafficking events and integrity of the various intracellular organelles located along the biosynthetic and endocytic pathways are coordinated and maintained by highly efficient and accurate control mechanisms.

Although the primary role of proteins in the control of membrane-trafficking events is indisputable, multiple studies indicate that lipids, in particular the highly phosphorylated metabolites of phosphatidylinositol (PtdIns), collectively called phosphoinositides (PI), also play a fundamental role (reviewed in Odorizzi *et al*., 2000; Corvera, 2001; Martin, 2001; Simonsen *et al*., 2001). Among the phosphoinositide species, the function of those phosphorylated at position D-3 of the inositol head group has been studied in more detail. The role of PtdIns 3-P has been first demonstrated by genetic studies in yeast that established the requirement for PtdIns 3-P kinase Vps34 in protein sorting and transport from the *trans*-Golgi to the vacuole (lysosome in higher cells) (Schu *et al*., 1993). Subsequent pharmacological studies with wortmannin, a relatively specific inhibitor of mammalian PI 3-kinase (PI 3-K) family members, demonstrated the requirement for PI 3-Ks in vesicular transport in mammalian cells. Wortmannin was found to exert numerous effects on endo-

Article published online ahead of print. Mol. Biol. Cell 10.1091/mbc.E03–04–0222. Article and publication date are available at www.molbiolcell.org/cgi/doi/10.1091/mbc.E03–04–0222.

‡ Corresponding author. E-mail: ashishev@med.wayne.edu

cytic and biosynthetic trafficking pathways in different cell types (Brown *et al*., 1995; Davidson, 1995; Martys *et al*., 1996; Shpetner *et al*., 1996; Spiro *et al*., 1996; Kundra and Kornfeld, 1998; Mills *et al*., 1999; Nordeng *et al*., 2002). Further studies to selectively target mammalian class IA or class III PI 3-Ks (most sensitive to wortmannin, low nanomolar concentrations; Fruman *et al*., 1998) by specific probes such as a dominant-negative kinase-deficient form of rVps34 (Row *et al*., 2001) or inhibitory antibodies against p110 catalytic subunits and hVps34 (Siddhanta *et al*., 1998; Futter *et al*., 2001) indicated the requirement for both class IA and class III PI 3-Ks in several but distinct transport steps. However, the inability of dominant-negative rVps34 or PI 3-K inhibitory antibodies to reproduce some of wortmannin-induced trafficking perturbations such as cathepsin D hypersecretion (Row *et al*., 2001) or the dramatic enlargement of late endocytic membranes (Futter *et al*., 2001) suggest other wortmannin-sensitive enzymes are also required.

A candidate lipid kinase involved in membrane-trafficking events in mammalian cells is PIKfyve (reviewed in Shisheva, 2001). The function of this enzyme is closely related to PI 3-K action in several ways. Thus, PIKfyve acts on PtdIns 3-P to generate PtdIns 3,5-P_2 (Sbrissa *et al*., 1999) and by this means, it likely functions downstream of PI 3-Ks, terminating the PtdIns 3-P signal, while initiating a new PtdIns 3,5-P_2 signal. Next, PIKfyve uses PtdIns 3-P for its localization on membranes of late endocytic compartments containing PtdIns 3-P (Sbrissa *et al*., 2002a). This association is promoted by the presence in PIKfyve of a FYVE finger domain (Shisheva *et al*., 1999), a protein module that specifically binds PtdIns 3-P (Gillooly *et al*., 2000). Consistent with the firm dependence of PIKfyve on PtdIns 3-P, we have recently identified association and cofractionation of PIKfyve with class IA PI 3-Ks at basal conditions by coimmunoprecipitation and density gradient centrifugation (Sbrissa *et al*., 2001). Immunofluorescence microscopy data colocalize a subset of membrane-bound PIKfyve with MPR but not with recycling transferrin (Tf), suggesting a role for PIKfyve in protein sorting and transport at later stages of the endocytic pathway (Shisheva *et al*., 2001). Consistent with this prediction, expression of lipid kinase-deficient point mutants ($PIKfyve^{K1831E}$ and $PIKfyve^{K1999E}$) elicited a dramatic dominant negative effect in the form of progressive accumulation of numerous swollen cytoplasmic vacuoles (Ikonomov *et al*., 2001, 2002a). This phenotype could be corrected by high levels of $PIKfyve^{WT}$ or microinjected PtdIns 3,5-P_2 but not by PtdIns 3-P, implying a selective role for PtdIns 3,5-P_2 in yet-to-be-identified steps of endosomal trafficking. Furthermore, studies with the PIKfyve ortholog Fab1p in yeast indicate the requirement of PtdIns 3,5-P_2 for inclusion of the vacuolar hydrolase carboxypeptidase S into vesicles that invaginate into the lumen of the endosomal compartment, forming multivesicular bodies (MVBs) (Odorizzi *et al*., 1998). Finally, it should be emphasized that wortmannin could influence PIKfyve function by several ways (mislocalization, substrate deprivation, and direct inhibition) consistent with the idea that the disturbed PIKfyve pathway and localized PtdIns 3,5-P_2 production account for some of the trafficking perturbations observed with wortmannin. Therefore, to test the role of PtdIns 3,5-P_2 in vesicle transport we have examined the effect of overexpression of $PIKfyve^{WT}$ or the dominant-negative kinase-deficient $PIKfyve^{K1831E}$ mutant in several trafficking assays of the recycling, endocytic, or biosynthetic pathways and inspected the organelle morphology by light, confocal, and electron microscopy.

MATERIALS AND METHODS

Cell Cultures

Stably transfected doxycycline-inducible TetOn human embryonic kidney (HEK) 293 clonal cells expressing $PIKfyve^{WT}$ (clone 9) or kinase-deficient dominant-negative $PIKfyve^{K1831E}$ (clone 5), generated by TetOff/TetOn gene expression systems (BD Biosciences Clontech, Palo Alto, CA), were characterized elsewhere (Sbrissa *et al*., 2002b). The stable HEK293 cell lines were maintained in DMEM containing 10% fetal bovine serum (FBS) and antibiotics: penicillin (50 U/ml), streptomycin sulfate (50 μg/ml), G418 (100 μg/ml), and hygromycin B (125 μg/ml). To induce PIKfyve protein expression, cells were seeded 18–36 h before experiments in the above-mentioned media, supplemented with doxycycline (1.0 μg/ml). To sustain multiple washes accompanying the trafficking assays, collagen IV-coated tissue culture dishes were used.

COS-7 cells seeded on glass coverslips (22 × 22 mm) were maintained in DMEM containing 10% FBS, penicillin (50 U/ml), and streptomycin sulfate (50 μg/ml).

Cell Metabolic Labeling and Cathepsin D Immunoprecipitation

Parental (TetOn), $PIKfyve^{WT}$ or $PIKfyve^{K1831E}$ HEK293 stable cell lines were grown to ~85% confluence on 60-mm dishes for 18 h in the presence of doxycycline to induce $PIKfyve^{WT}$ or $PIKfyve^{K1831E}$ expression. Cells were then washed twice with phosphate-buffered saline (PBS) and incubated for 1 h at 37°C in serum-free, methionine-free DMEM, supplemented with 4 mM glutamine and 2 mM pyruvate. Cells were metabolically labeled for 30 min at 37°C with 200 μCi/ml Express [^{35}S]methionine/cysteine protein labeling mix (PerkinElmer Life Sciences, Boston, MA) in the above-mentioned medium supplemented with 20 mM HEPES, pH 7.4. Cells were then chased in a complete medium supplemented with 20 mM HEPES, pH 7.4, and 1 mM methionine for time periods indicated in the figure. Where indicated, wortmannin (3 μM) was present during the chase. Cells were washed twice in PBS and then scraped in radioimmunoprecipitation assay (RIPA) buffer supplemented with 1× protease inhibitor cocktail (1 mM phenylmethylsulfonyl fluoride, 5 μg/ml leupeptin, 5 μg/ml aprotinin, 1 μg/ml pepstatin, and 1 mM benzamidine). Cell lysates, clarified by centrifugation (15 min, 4°C) and media from the individual culture dishes (supplemented with the above-mentioned inhibitors) were immunoprecipitated (18 h, 4°C) with affinity-purified anti-cathepsin D polyclonal antibodies (10 μg/60-mm dish), a kind gift from Dr. G. Conner. Protein A-Sepharose CL-4B beads were added at 4°C during the last 90 min of incubation. Immunoprecipitates were washed in RIPA buffer and resolved by SDS-PAGE. Proteins were transferred onto a nitrocellulose membrane and analyzed by autoradiography (Kodak X-Omat AR film; Eastman Kodak, Rochester, NY). The same filters were immunoblotted with an anti-cathepsin D monoclonal antibody (Calbiochem, San Diego, CA) to confirm the identity of the cathepsin D radioactive bands. In some experiments, gels were dried and subjected to autoradiography without prior protein transfer.

Horseradish Peroxidase (HRP) Endocytosis

Uptake of the fluid phase marker HRP was determined in the parental or stably transfected $PIKfyve^{WT}$ and $PIKfyve^{K1831E}$ HEK293 cell lines, seeded in the presence of doxycycline to induce PIKfyve expression (triplicate 35-mm dishes/condition). Thirty-six hours postinduction, cells (80% confluence) were washed with Dulbecco's phosphate buffered saline (DPBS, Ca^{2+} and Mg^{2+} free) and then incubated at 37°C with HRP (2 mg/ml) in DMEM, containing 0.1% bovine serum albumin and 10 mM HEPES, pH 7.4, for the time periods indicated in the figures. Dishes were placed on ice, washed four times with ice-cold DMEM, supplemented with 10 mM HEPES, pH 7.4, and five times with DPBS. Cells were scraped at 4°C with DPBS, containing 1% Triton X-100. After centrifugation in a Microfuge for 10 min at 4°C, aliquots of the supernatants were processed by 1-Step Turbo TMB enzyme-linked immunosorbent assay kit (Pierce Chemical, Rockford, IL). HRP activity was read at an absorbance of 450 nm (DU-50 spectrophotometer; Beckman Coulter, Fullerton, CA) subsequent to 20-min incubation at 37°C with the substrate. The activity was normalized per protein content (bicinchoninic acid protein assay kit; Pierce Chemical).

Transferrin Internalization, Recycling, and Internalized to Surface (IN/SUR) Analysis

Human holotransferrin (iron saturated; Sigma-Aldrich) was iodinated with [^{125}I]NaI (PerkinElmer Life Sciences) and Iodogen (Pierce Chemical), following the manufacturer's protocol, and then purified on a Sephadex G-15 column. To measure the rate of Tf uptake, stably transfected or parental cell lines, seeded on 35-mm dishes (triplicate dishes/condition) in the presence of doxycycline for 18 h were washed in DPBS and incubated in depletion media (DMEM, supplemented with 0.2% bovine serum albumin, 20 mM HEPES, pH 7.4) at 37°C for 2 h to remove endogenous Tf. Cells were then incubated in a new portion of the same media supplemented with ^{125}I-holotransferrin (25

μM) for the time intervals indicated in the figures. Dishes were then placed on ice and cells were washed twice with ice-cold Solution 1 (20 mM HEPES, pH 7.4, 150 mM NaCl, 1 mM $CaCl_2$, 5 mM KCl, 1 mM $MgCl_2$) and once with an acid solution (0.2 N acetic acid, 0.2 M NaCl) for 2 min at 4°C to remove surface-bound Tf. Cells were rewashed with ice-cold solution 1 and then solubilized in 0.1% Triton X-100/0.1 N NaOH in PBS. The incorporated radioactivity was measured by gamma counting. To measure the Tf recycling, cells were first incubated in depletion media as described above and then for an additional 60 min in media supplemented with ^{125}I-Tf (2.5 μM). Cells were placed on ice and rinsed once with solution 1 at 4°C. The recycling was measured by cell incubation in depletion media supplemented with nonlabeled Tf (100 μM). At indicated time points, the media were collected to measure the released radioactivity. Cells were acid washed for 2 min at 4°C to strip the surface-bound ^{125}I-Tf and after an additional wash in solution 1, cells were lysed in 0.1% Triton X-100/0.1 N NaOH in PBS to determine the incorporated radioactivity. To determine the ratio of IN/SUR transferrin (Wiley and Cunningham, 1982), cells were allowed to take up ^{125}I-Tf (25 μM) for 1–10 min as described above. At the indicated time intervals, duplicate samples were quenched in parallel to measure total and internal ^{125}I-Tf. The total cell-associated radioactivity was counted in the solubilized cells subsequent to three washes in solution 1. For measuring the internal ^{125}I-Tf, cells received a 2-min acid wash at 4°C before washes in solution 1 and lyses in 0.1% Triton X-100/0.1 N NaOH as described above. Surface-bound ligand was calculated as the difference between total and intracellular radioactivity measured in the parallel samples.

Epidermal Growth Factor Receptor (EGFR) Degradation

EGFR degradation was determined in the parental or stably transfected PIKfyve^{WT} and PIKfyve^{K1831E} HEK293 cell lines, seeded in the presence of doxycycline (duplicate 60-mm dishes/condition). Eighteen hours postinduction, cells were serum starved for 6 h in DMEM and then stimulated with epidermal growth factor (EGF) (100 μg/ml). At the indicated time points, the cells were collected in RIPA buffer, supplemented with 1× protease inhibitor cocktail and 2 mM sodium orthovanadate. Equal protein amounts were subjected to SDS-PAGE (6% gel), and after protein transfer, the membranes was blocked under previously specified conditions (Sbrissa *et al*., 1999) and then blotted with monoclonal EGFR antibody (antibody-12; NeoMarkers, Fremont, CA). After washes, bound antibody was detected with horseradish peroxidase-bound anti-mouse IgG and a chemiluminescence kit (Pierce Chemical).

Transient Cell Transfection, Fluorescence, and Immunofluorescence Microscopy

COS-7 cells were seeded on 22- × 22-mm coverslips (35-mm dishes) and transfected with pEGFP-HA-PIKfyve^{K1831E} cDNA (Shisheva *et al*., 2001) by using LipofectAMINE (Invitrogen, Carlsbad, CA) as a transfection reagent. Twenty-four hours posttransfection, the cells were incubated with Texas Red (TxR)-Tf (8 μg/ml; Molecular Probes, Eugene, OR) in serum-free, dye-free DMEM for 60 min at 37°C to visualize the recycling pathway by steady-state Tf uptake. Dishes were then placed on ice, cells were washed with ice-cold PBS, and fixed for 1 h at 4°C in formaldehyde (4% in PBS) before rewashing and mounting. To visualize the fluid phase endocytic pathway, transfected cells were incubated with TxR-conjugated dextran (size 10,000, 1 mg/ml; Molecular Probes) in DMEM (dye-free) containing 10% FBS for 2 h at 37°C. Cells were then washed with ice-cold PBS, fixed for 15 min at 25°C in paraformaldehyde (3.7% in PBS), rewashed, and mounted. End lysosomes were visualized by incubating transfected cells with TxR-conjugated dextran in DMEM containing 10% FBS for 16 h at 37°C. Cells were then chased for 2 h in dextran-free medium, and after washes in PBS, were fixed for 15 min at 25°C in paraformaldehyde, rewashed and mounted. Double labeling with anti-cation-independent MRP (gift from Dr. B. Hofflack, Institute Pasteur, Lille, France), anti-β-COP (gift from Dr. E. Tisdale, Wayne State University, Detroit, MI), or anti-TfR antibodies (gift from Dr. I. Trowbridge, The Salk Institute, San Diego, CA) was performed subsequent to formaldehyde fixation and cell permeabilization with 0.5% Triton X-100 in PBS plus 1% FBS. Primary antibodies were detected by CY3-coupled goat anti-rabbit IgG (Kirkegard and Perry Laboratories, Gaithersburg, MD) or TxR-coupled goat anti-mouse IgG (Molecular Probes), as detailed elsewhere (Shisheva *et al*., 2001). Coverslips were mounted on slides and observed on a confocal microscope (LSM 310; Carl Zeiss, Thornwood, NY) by using a 63/1.4 oil immersion lens.

Light and Electron Microscopy

Light microscopy of live HEK293 cell lines was performed with a digital imaging fluorescence microscope (Eclipse TE200; Nikon, Tokyo, Japan) by using a 40× Hoffman modulation contrast objective. Representative images were captured by a SPOT Slider charge-coupled-device camera and processed further by SPOT 3.2 software. For transmission electron microscopy analyses, stably transfected PIKfyve^{WT} or PIKfyve^{K1831E} HEK293 cell lines as well as the parental HEK293 cells were grown on 100-mm dishes and treated with doxycycline for 36 h. Cells were then washed in a 0.1 M sodium phosphate buffer, pH 7.5, and fixed with 2.5% glutaraldehyde for 2 h at room temperature. Cells were then dehydrated and processed for electron microscopy as described previously (Carpentier *et al*., 1978). Thin sections were examined in a Philips (Eindhoven, The Netherlands) CM10.

RESULTS

Processing and Delivery of Newly Synthesized Lysosomal Enzymes Is Unaffected by PIKfyve Enzymatic Activity

One of the most prominent outcomes of wortmannin inhibition is abnormal processing and hypersecretion of newly synthesized procathepsin D demonstrated in several mammalian cell types (Brown *et al*., 1995; Davidson, 1995). Because PtdIns 3,5-P_2 is generated from PtdIns 3-P, it is conceivable that through inhibiting the PtdIns 3-P-producing kinases, wortmannin deprives PIKfyve of PtdIns 3-P substrate and the reduced PtdIns 3,5-P_2 levels account for the observed effect. To address the role of PtdIns 3,5-P_2 production in the sorting of lysosomal enzymes, we have examined the role of PIKfyve^{WT} or a dominant-negative kinase-deficient PIKfyve^{K1831E} mutant in cathepsin D transport in HEK293 stable cell lines. Previous studies in other cell types have shown that cathepsin D is initially synthesized as a ~53 kDa unprocessed form, which persists as the protein passes through the secretory compartments to TGN (Rijnboutt *et al*., 1992, Brown *et al*., 1995; Davidson, 1995). After delivery to the prelysosomal compartment, procathepsin D undergoes a proteolytic processing step to yield a 47-kDa intermediate form. After reaching lysosomes, procathepsin D undergoes a second proteolytic cleavage to form the mature enzyme comprising noncovalently associated 31- and 14-kDa polypeptides (Rijnboutt *et al*., 1992; Brown *et al*., 1995; Davidson, 1995). Consistent with these observations, our control pulse-chase experiments in parental TetOn HEK293 cells have demonstrated a similar pattern and kinetics of procathepsin D maturation both in the presence or absence of doxycycline with no detectable enzyme secretion in the culture medium over a chase period of 3 h (Figure 1A). In contrast, wortmannin treatment of these cells resulted in procathepsin D hypersecretion (Figure 1A) in agreement with previous studies (Brown *et al*., 1995; Davidson, 1995). We next examined the processing and transport of cathepsin D in HEK293 stable cell lines induced to express PIKfyve^{WT} or dominant-negative kinase-deficient PIKfyve^{K1831E} mutant by doxycycline. Western blot analysis of lysates from these cells demonstrated significant levels of both the wild-type and the mutant protein expression that exceeded by sevenfold the endogenous PIKfyve levels upon 18-h induction with doxycycline (Sbrissa *et al*., 2002b). Examination of cell morphology by light microscopy documented a dramatic endomembrane swelling and vacuolation 18 h postinduction of PIKfyve^{K1831E} expression (Figure 2), similar to that observed previously in other cell types transiently expressing this mutant (Ikonomov *et al*., 2001). In contrast, induction of PIKfyve^{WT} expression was without apparent phenotype (Figure 2) consistent with our previous observations in other cells transiently expressing the wild-type (Ikonomov *et al*., 2001). Under these conditions (18-h postinduction), the cell lines were pulse labeled for 30 min, chased for 0/180 min, and after cathepsin D immunoprecipitation from both cell lysates and culture media, the SDS-PAGE–resolved immunoprecipitates were analyzed by autoradiography. As illustrated in Figure 1B, expression of both the active or inactive PIKfyve enzyme produced similar pattern and kinetics of procathepsin D intracellular maturation resembling those observed in the parental TetOn HEK293 (Figure 1A). Thus, a

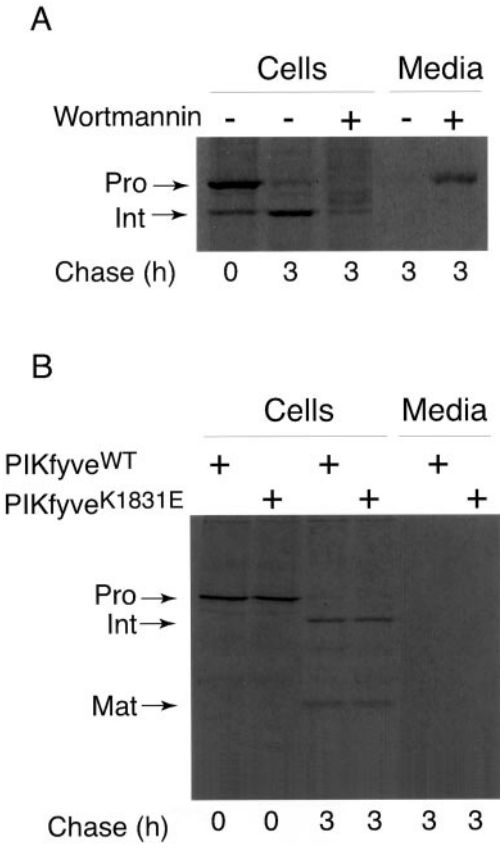

Figure 1. Normal sorting of procathepsin D in the presence of PIKfyve^{K1831E} or PIKfyve^{WT} expression in HEK293 stable cell lines. (A) Control TetOn HEK293 stable cell line was pulse-labeled with [^{35}S]methionine as described under MATERIALS AND METHODS. Cells were then chased for indicated times in the presence or absence of wortmannin (3 μM; freshly added every 40 min during chase). Cells and media were collected, and cathepsin D was immunoprecipitated. Proteins were resolved by SDS-PAGE and the dried gel was subjected to autoradiography. Shown is an autoradiogram from a representative experiment of two with similar results. (B) PIKfyve^{WT} or PIKfyve^{K1831E}-expressing HEK293 stable cell lines were pulse-labeled as described in A and chased for the indicated time. Cathepsin D was immunoprecipitated and analyzed as specified above. Shown is an autoradiogram from a representative experiment of five with similar results. Positions of the 53-kDa procathepsin D (Pro), the 47-kDa intermediate (Int), and the mature (Mat) 31-kDa forms are indicated.

53-kDa procathepsin D was detected at the beginning of the chase (Figure 1B). After a 180-min chase period, ~90% of the newly synthesized immunoprecipitable cathepsin D was found as processed 47-kDa intermediate and 31-kDa mature forms that were present in almost equal amounts (Figure 1B). Neither one of the cathepsin D forms were secreted in the medium at detectable levels at any time point during the 180-min chase period (Figure 1B; our unpublished data). These results demonstrate a normal processing and transport of newly synthesized procathepsin D in the presence of both expressed PIKfyve^{WT} or dominant-negative PIKfyve^{K1831E}, consistent with the conclusion that PIKfyve enzymatic activity, and therefore PtdIns 3,5-P_2 are irrelevant in the sorting of newly synthesized lysosomal enzymes from TGN to lysosomes. In addition, our results show normal processing in the Golgi/prelysosomal compartments and lysosomal targeting of newly synthesized acid hydrolases despite the presence of dramatic PIKfyve^{K1831E}-dependent endomembrane swelling, implying that the procathepsin D hypersecretion observed in response to wortmannin (Brown *et al*., 1995; Davidson, 1995; Figure 1A) is not secondary to the abnormal morphology induced by the inhibitor. Rather, it involves yet another wortmannin-sensitive enzyme distinct from hVPS34 (Row *et al*., 2001) and PIKfyve (this study). Thus, although endomembrane vacuolation is induced by both wortmannin and PIKfyve^{K1831E}, only the former affects procathepsin D sorting and targeting to the endocytic pathway.

Late Fluid Phase Endocytosis Is Inhibited by Dominant-Negative PIKfyve

Prelysosomal compartments also receive internalized materials from the cell surface that are destined for degradation in lysosomes. We first tested whether PIKfyve enzymatic activity functions in the fluid phase endocytosis by examining the uptake of HRP, a fluid phase marker that reaches lysosomes by fluid phase endocytosis. In parental HEK293 cells treated with doxycycline, the uptake of HRP was found to increase proportionally with time up to the 90th min of uptake (Figure 3). The HEK293 stable cell line induced to express PIKfyve^{WT} demonstrated a rate of uptake of the fluid phase marker similar to that observed in the parental cells (Figure 3). In contrast, HRP endocytosis was inhibited in HEK293 cell line expressing the PIKfyve^{K1831E} mutant. This inhibitory effect was markedly pronounced at later uptake times with amounts of internalized HRP being reduced up to fourfold at the 90th-min versus the parental or PIKfyve^{WT}-expressing HEK293 cells (Figure 3). Intriguingly, at the earlier uptake times (up to 10 min) the rate of HRP internalization in PIKfyve^{K1831E}-expressing cells was comparable with that detected in the parental or PIKfyve^{WT}-expressing HEK293 cells, indicating that the initial rate of fluid phase endocytosis remained largely unaltered by the mutant protein.

Receptor-mediated Endocytosis and Recycling of Transferrin Is Unaffected by PIKfyve Enzymatic Activity

Having established that expression of the PIKfyve^{K1831E} mutant inhibits later, but not earlier steps in the endocytic pathway of fluid phase markers, we next examined whether receptor-mediated endocytosis and recycling were affected. We measured the rate of internalization and recycling of surface-bound ^{125}I-labeled Tf, a cycle that has been previously characterized in numerous cell types. In the internalization protocol, the stably transfected HEK293 cells induced to express either PIKfyve^{WT} or PIKfyve^{K1831E} for 18 h, were allowed to internalize ^{125}I-Tf for the indicated time periods (Figure 4A). At each time point, cell surface-bound ^{125}I-Tf was stripped by an acid wash and the internalized ^{125}I-Tf determined in the cell lysates. As illustrated in Figure 4A, expression of PIKfyve^{WT} or PIKfyve^{K1831E} shows similar rates of intracellular accumulation of ^{125}I-Tf. Data obtained for the initial time periods of internalization in these experiments, when plotted as a ratio of internalized to cell surface bound ^{125}I-Tf (IN/SUR), also yielded lines with similar slopes (Figure 4A, inset). To evaluate Tf exocytosis, the cells were first incubated with ^{125}I-Tf and then chased with unlabeled Tf for the indicated time periods. Data presented in Figure 4B demonstrate that the rate of transferrin receptor exocytosis was similar between the cells expressing PIKfyve^{WT} and PIKfyve^{K1831E}. Together, the data demonstrate that neither the rate of ^{125}I-Tf uptake nor the release of internalized radiolabeled Tf were significantly altered by

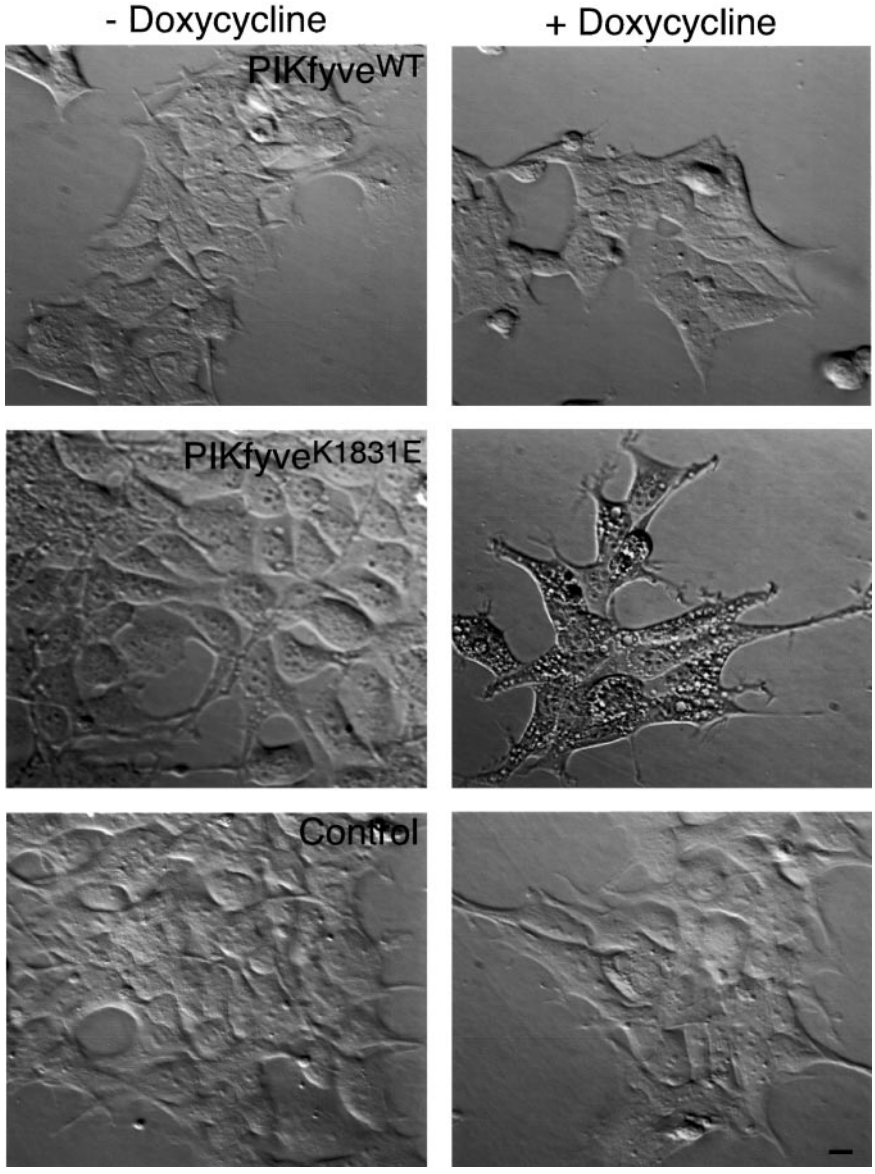

Figure 2. TetOn-induced expression of PIKfyve^{K1831E} but not that of PIKfyve^{WT} is associated with appearance of multiple cytoplasmic vacuoles. Indicated HEK293 cell lines, stably expressing HA-PIKfyve^{WT} (clone 9), HA-PIKfyve^{K1831E} (clone 5), or control TetOn were seeded in the presence or absence of doxycycline as described under MATERIALS AND METHODS. Eighteen hours postinduction of protein expression, cells were observed live with a TE200 microscope (Nikon), and images were captured by a SPOT RT Slider camera. Bar, 10 μm.

PIKfyve^{WT} or PIKfyve^{K1831E} expression, consistent with the hypothesis that PIKfyve activity is not a part of the mechanisms that operate in receptor-mediated endocytosis and recycling.

EGFR Degradation Is Unaltered by PIKfyve^{K1831E} Expression

Having established that PIKfyve enzymatic activity does not alter the rate of receptor-mediated endocytosis and recycling, we next tested whether receptor trafficking to lysosomes was affected. This is particularly intriguing given the fact that HRP sorting into the lysosomal pathway was found to be profoundly affected, as discussed above. As a marker, we examined the degradation efficiency of endogenous EGFR, which is delivered to lysosomes after EGF-induced receptor internalization and sorting in MVBs (Futter *et al.*, 2001). The three stable cells lines, seeded on doxycycline-supplemented media to induce protein expression, were serum-deprived and after cell stimulation with EGF for indicated times (Figure 5), the EGFR levels were determined by Western blotting with anti-EGFR monoclonal antibody. In both control and PIKfyve^{WT}-expressing HEK293 cell lines, we observed a similar decrease in the immunoreactive EGFR signal over time consistent with the receptor degradation upon ligand stimulation (Figure 5). More importantly, EGFR underwent a similar degradation efficiency upon EGF stimulation of the PIKfyve^{K183E}-expressing HEK293 cell line (Figure 5). Thus, in contrast to the dramatic effect of PIKfyve^{K1831E} on HRP endocytosis, EGFR internalization into the degradation pathway was not significantly affected.

PIKfyve^{K1831E} Expression Disrupts the Late Endocytic Compartment

To characterize the effect of PIKfyve^{K1831E} expression on the morphology of organelles involved in the endocytic and biosynthetic pathways examined above by biochemical assays, we used confocal microscopy to monitor COS cells,

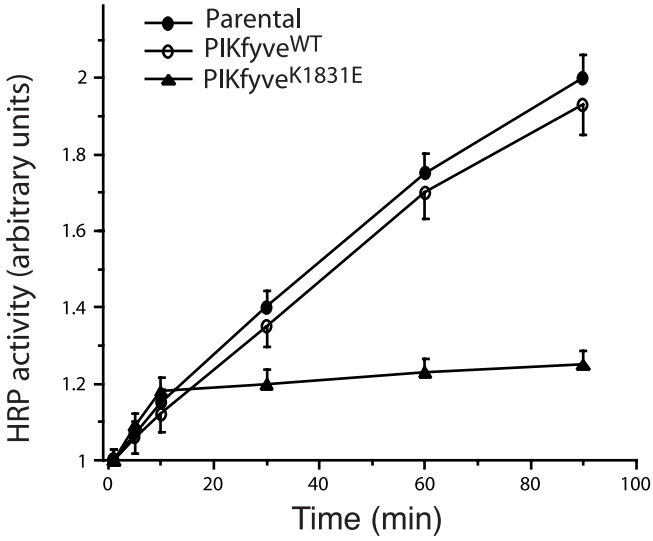

Figure 3. Expression of PIKfyve^{K1831E} but not that of PIKfyve^{WT} inhibits later stages of HRP uptake in HEK293 stable cell lines. Indicated cell lines were seeded in the presence of doxycyline as described under MATERIALS AND METHODS. Eighteen hours postinduction of protein expression, cells were incubated in the presence of 2 mg/ml HRP for the indicated time periods. Washed cells were lysed, and HRP activity was read at an absorbance of 450 nm subsequent to 20-min incubation with TMB substrate. Data shown are normalized for protein content and are presented relatively to the HRP activity determined at the 1-min incubation period for each cell line. The data represent the mean ± SEM from three independent experiments in triplicates.

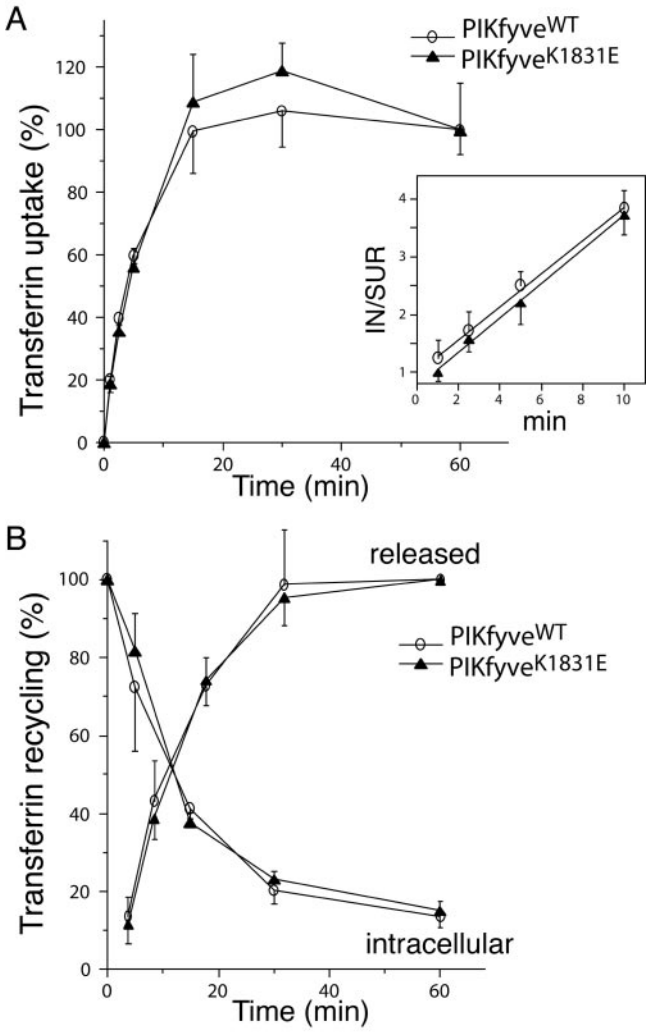

Figure 4. Uptake and recycling of Tf are not affected by expression of PIKfyve^{K1831E} or PIKfyve^{WT} in HEK293 stable cell lines. Indicated cell lines were seeded in the presence of doxycycline. Eighteen hours postinduction of protein expression, cells were incubated in the presence of ^{125}I-Tf at 37°C for the indicated time intervals (A) or for 60 min (B) as detailed under MATERIALS AND METHODS. (A) Cells were washed, surface-bound ^{125}I-Tf was stripped by an acid wash, and the incorporated radioactivity was determined in the cell lysates. Shown is a quantitation from three independent experiments (each in triplicate) expressed as a percentage of the acid-resistant cell-incorporated radioactivity of the 60-min point for each cell line. Inset, IN/SUR analysis was performed in two duplicate sets of samples subsequent to determination of internalized and total radioactivity respectively, as described in MATERIALS AND METHODS. (B) At the end of the 60-min incubation with ^{125}I-Tf, cells were washed to eliminate unbound ligand and then chased with unlabeled Tf for the indicated time intervals. Media were then collected to determine the released radioactivity. Cells were washed, the surface-bound ligand was stripped by an acid wash, and the incorporated radioactivity was determined in the cell lysates. Shown is a quantitation from three independent experiments (in triplicate) expressed as a percentage of the 1-min value (intracellular) or 60-min value (released) for each cell line.

transiently transfected with PIKfyve^{K1831E}. We used a transient transfection system because it allows a direct comparison of organelle morphology between transfected and the neighboring nontransfected cells in the same field, and selected COS cells for these experiments due to their larger size. It should be emphasized, however, that like in the HEK293 stable line, transient overexpression of the PIKfyve^{K1831E} mutant in COS cells is associated with morphological changes in the form of similar endomembrane swelling, as we have previously shown, and confirmed here (Ikonomov *et al*., 2001, and Figure 6, b, e, h, k, and n). Visualization of early endocytic and recycling compartments by both TxR-derivatized Tf at steady state (60-min uptake; Figure 6a) or anti-TfR (our unpublished data) demonstrated the characteristic intracellular distribution of TfR in both nontransfected and PIKfyve^{K1831E}-expressing cells. As illustrated in Figure 6a, steady-state labeling visualizes the fluorescence signals of derivatized Tf predominantly in the juxtanuclear region, which represents the recycling endosomes (Mayor *et al*., 1993; Hopkins *et al*., 1994). A similar pattern for TfR distribution is seen in PIKfyve^{K1831E}-transfected cells, despite the formation of numerous enlarged cytoplasmic vacuoles due to PIKfyve^{K1831E} expression (Figure 6, a–c). Thus, the lack of substantial functional changes in the rate of Tf endocytosis and recycling upon expression of PIKfyve^{K1831E} correlates with the lack of gross morphological abnormalities in the recycling endosomes defined by TfR.

The structure of the endocytic pathway was further evaluated by continuous labeling of the endosomal system with the fluid phase marker TxR-dextran for a 120-min internalization period. Under these conditions, the marker stains a heterogeneous population of endosomal membranes along the endocytic pathway, the most prominent being postendosomal/prelysosomal/lysosomal compartments. As illustrated in Figure 6d, the structures stained by TxR-dextran in the nontransfected cells are vesicular in appearance with

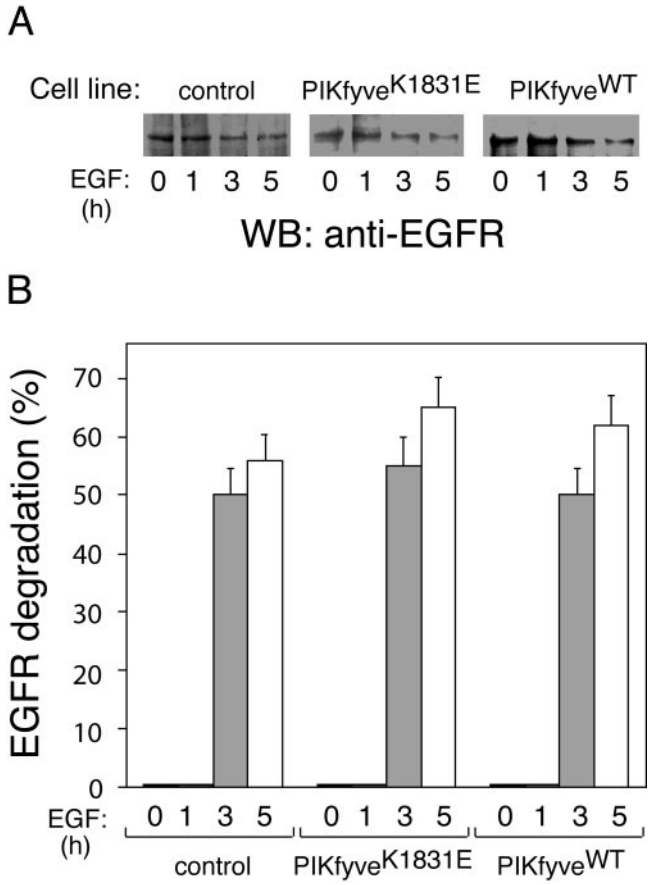

Figure 5. Normal rate of EGFR degradation in the presence of expressed PIKfyve^{K1831E} or PIKfyve^{WT}. Indicated cell lines were seeded in the presence of doxycycline. Eighteen hours postinduction of protein expression, serum-starved cells were stimulated with EGF for the indicated time periods. Cell lysates were clarified and analyzed by immunoblotting with anti-EGFR antibody. Shown are chemiluminescence detections of representative immunoblots (A) and a quantitation of EGFR degradation from two independent experiments in duplicates expressed as a percentage of the total EGFR at the 0 min of each cell line (B).

more concentrated signals in the perinuclear region of the cells. However, in cells expressing PIKfyve^{K1831E} the TxR-dextran-positive structures displayed a markedly different staining pattern. Instead of the typical perinuclear concentration, seen in nontransfected cells, the TxR-dextran–positive vesicles appeared dispersed throughout the cytoplasm, often swollen and enlarged (Figure 6, d–f). The fluorescence associated with the fluid phase marker was typically not detectable within the lucent vacuoles but rather among them (Figure 6f). Conditions such as an overnight application of the fluid phase marker followed by 2-h chase allow TxR-dextran to accumulate in end lysosomes. This approach showed that the fluorescence appearance of the end lysosomes was not significantly affected by expression of PIKfyve^{K1831E} mutant; transfected and nontrasfected cells displayed very similar patterns (Figure 6, g–i). Collectively, the results of these experimental approaches indicate that the integrity of the postendosomal/prelysosomal compartments of the endocytic pathway, but not the end lysosomes, defined by the fluid phase marker dextran were substantially disrupted in the PIKfyve^{K1831E}-expressing cells.

The structure of the biosynthetic pathway was evaluated in transfected and nontransfected COS cells by examining the immunofluorescence profiles associated with the Golgi marker β-COP. Consistent with previous studies, a characteristic intense juxtanuclear staining of Golgi structures was documented in the nontransfected cells. Intriguingly, observation of the PIKfyve^{K1831E}-transfected cells demonstrated a similar pattern of β-COP distribution despite the drastic morphological changes in these cells (Figure 6, j–l). The morphology of the biosynthetic pathway was further examined by monitoring CI-MPRs, which sort and transport newly synthesized lysosomal enzymes from TGN to late endosomes and are distributed between those compartments (Griffiths *et al.*, 1990). As illustrated in Figure 6, m–o, in nontransfected cells the immunofluorescence associated with CI-MPR is observed in discrete vesicular elements in the peripheral cytoplasm with a high focal concentration at the juxtanuclear region. PIKfyve^{K1831E}-expressing cells displayed a more densely clustered perinuclear appearance of the MPR immunofluorescence signals, with vesicles typically retracted from the cell periphery, and, sometimes, with an enlarged appearance (Figure 6, m–o).

To obtain information on morphological abnormalities induced upon expression of PIKfyve^{K1831E}, we have next examined HEK293 stable lines at the ultrastructural level. Electron microscopy analyses of Epon-embedded thin sections of HEK293 cells expressing PIKfyve^{WT} and PIKfyve^{K1831E} revealed striking differences in the size and morphology of MVB structures. In the parental or PIKfyve^{WT}-expressing HEK293 cell lines, MVBs appeared as relatively dense round structures of 0.2- to 1-μm diameter, in which lumen numerous small vesicles and multilamellar membranes (membrane whorls) could be seen (Figure 7, C and D). In contrast, the PIKfyve^{K1831E}-expressing cells displayed large swollen vacuoles of 0.6- to 2.1-μm diameter observed throughout the cytoplasm (Figure 7A), consistent with the findings by light microscopy (Figure 2). These enlarged structures were reminiscent of MVBs because they still contained some intralumenal vesicles or membrane whorls (Figure 7, A and B), although significantly less in number compared with the MVB lumenal membranes in control HEK293 cells or those expressing PIKfyve^{WT} (Figure 7, C and D). These results demonstrate a dramatic morphological perturbation in MVB-like structures upon expression of kinase-deficient PIKfyve^{K1831E}, suggesting that the mechanisms of MVB morphogenesis require intact PIKfyve enzyme and PtdIns 3,5-P_2 production.

DISCUSSION

The present study was undertaken to analyze the role of PtdIns 5-P/PtdIns 3,5-P_2–synthesizing enzyme PIKfyve in the membrane-trafficking events in mammalian cells. To this end, we used stably transfected HEK293 cell lines, inducibly expressing PIKfyve^{WT} or a dominant-negative kinase-deficient PIKfyve^{K1831E} mutant, to assess the performance of several trafficking pathways and to obtain information about organelle morphology. The key finding we document here is that induced expression of PIKfyve^{K1831E} inhibits sorting of fluid phase markers in the degradative arm of the endocytic pathway but it has no detectable effects on the sorting of Tf for recycling to the plasma membrane, the sorting of EGFR for degradation in lysosomes, or the sorting of procathepsin D from the secretory pathway to lysosomes. The data from both the functional assessment of trafficking pathways by

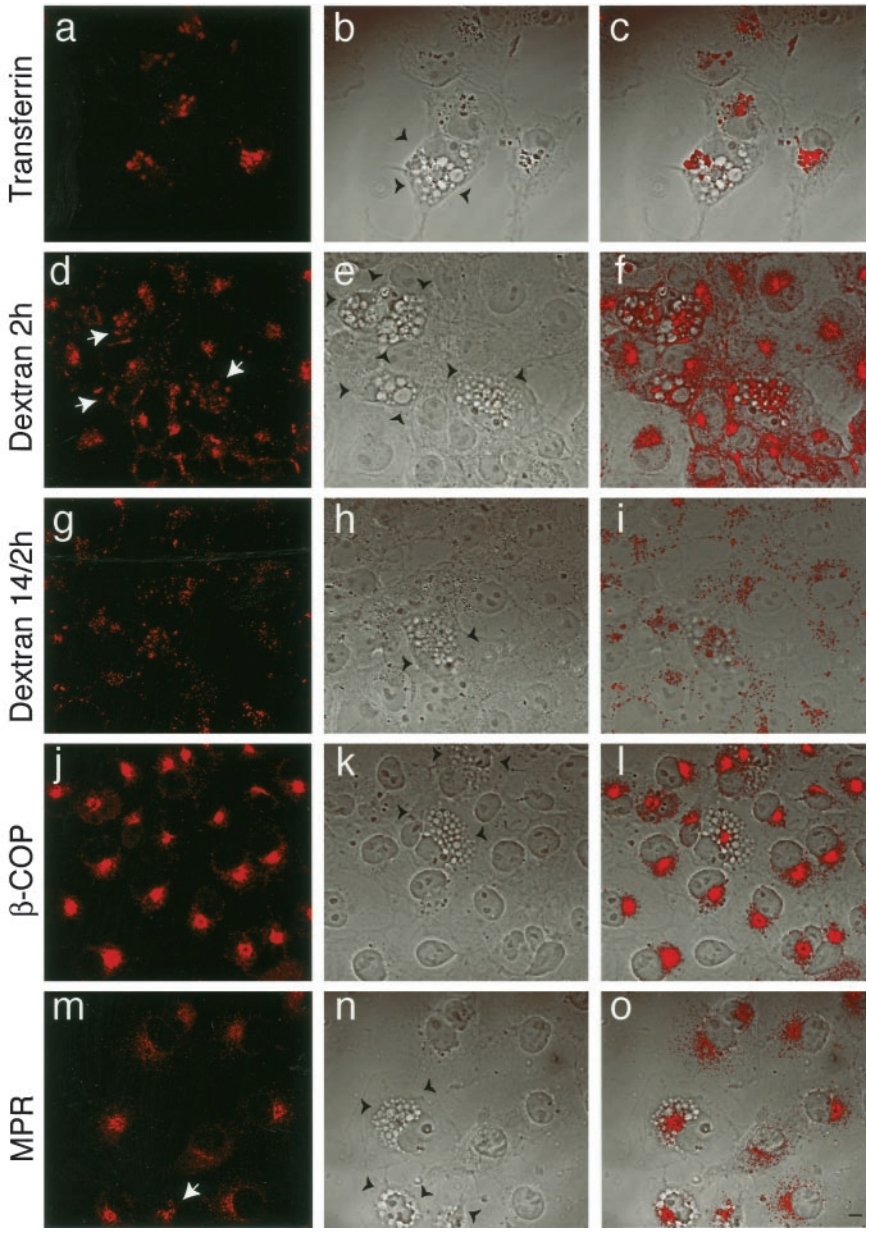

Figure 6. Effect of PIKfyve^{K1831E} expression on organelle morphology. Eighteen hours post-transfection with pEGFP-HA-PIKfyve^{K1831E} cDNA, COS-7 cells were processed for indirect immunofluorescence or fluorescence microscopy as described under MATERIALS AND METHODS. a, the recycling compartment was visualized by incubating cells with TxR-Tf for 60 min at 37°C. Apparent is the similar pattern of TfR distribution in transfected and nontransfected cells; d, cells were incubated for 120 min at 37°C with the fluid phase marker TxR-dextran to label the structure of the endocytic pathway. Instead of the typical perinuclear concentration, seen in nontransfected cells, the TxR-dextran-positive vesicles seemed dispersed throughout the cytoplasm, swollen, and enlarged (arrows); g, cells were incubated for 14 h at 37°C with the fluid phase marker TxR-dextran and then chased for 2 h to label end lysosomes. Transfected and nontransfected cells show similar pattern of end lysosome appearance; j, fixed and permeabilized cells were successively incubated with anti-β-COP antibodies and CY3-coupled goat anti-rabbit IgG, to visualize the Golgi apparatus; m, fixed and permeabilized cells were successively incubated with anti-MPR antibodies and CY3-coupled goat anti-rabbit IgG, to visualize MPR-containing compartments. Apparent is the more tightly concentrated perinuclear appearance of the MPR immunofluorescence signals in the PIKfyve^{K1831E}-expressing cells, with vesicles retracted from the periphery, sometimes enlarged (arrows). The pEGFP-HA-PIKfyve-transfected cells are identified by both phenotypic changes seen on phase contrast images b, e, h, k, and n of the fields presented in images a, d, g, j, and m, respectively, and fluorescence signals of GFP (our unpublished data) and are outlined by black arrowheads in b, e, h, k, n. Cells on the right (c, f, i, l, o) are the overlay of the two left images and demonstrate the organelle morphology relative to the vacuoles observed in the PIKfyve^{K1831E}-expressing cells. Bar, 10 μm.

biochemistry and morphological inspection of the organelles by confocal microscopy are consistent with the role of PIKfyve enzymatic activity and PtdIns 3,5-P_2 production in the fluid phase endocytic pathway at the level of postendosomal-prelysosomal compartments. The fluid phase marker was still able to reach the lysosomes after a longer incubation period, consistent with the notion that impaired PIKfyve activity imposes a kinetic rather than an absolute block on fluid phase endocytic transport. Furthermore, the ultrastructural information in PIKfyve^{K1831E}-expressing cells visualizing the formation of swollen MVB-derived vacuoles with reduced number of lumenal vesicles and membrane whorls provides a potential mechanism to explain the observed block in endocytic traffic. The substantial loss of accumulated lumenal vesicles and membrane whorls indicates the requirement for active PIKfyve and PtdIns 3,5-P_2 production in MVB morphogenesis.

PIKfyve Activity Is the Key PI 3-K Downstream Effector in MVB Morphogenesis

A hallmark of the MVBs/late endocytic compartment is the presence of internal membrane structures in the form of small vesicles and membrane whorls (Piper and Luzio, 2001). This characteristic feature was also documented here in HEK293 stable cells expressing PIKfyve^{WT} by electron microscopy (Figure 7). The molecular mechanisms that lead to accumulation of lumenal membranes, a process that likely starts at the early endosomes and continues as the endosomes mature to late endosomes/MVBs, are poorly understood. Previous studies with wortmannin have documented a massive accumulation of swollen endosomes in different cell types, suggesting a role of PI 3-Ks in this process. Based on electron microscopy assessment of the enlarged endocytic compartments in wortmannin-treated cells several

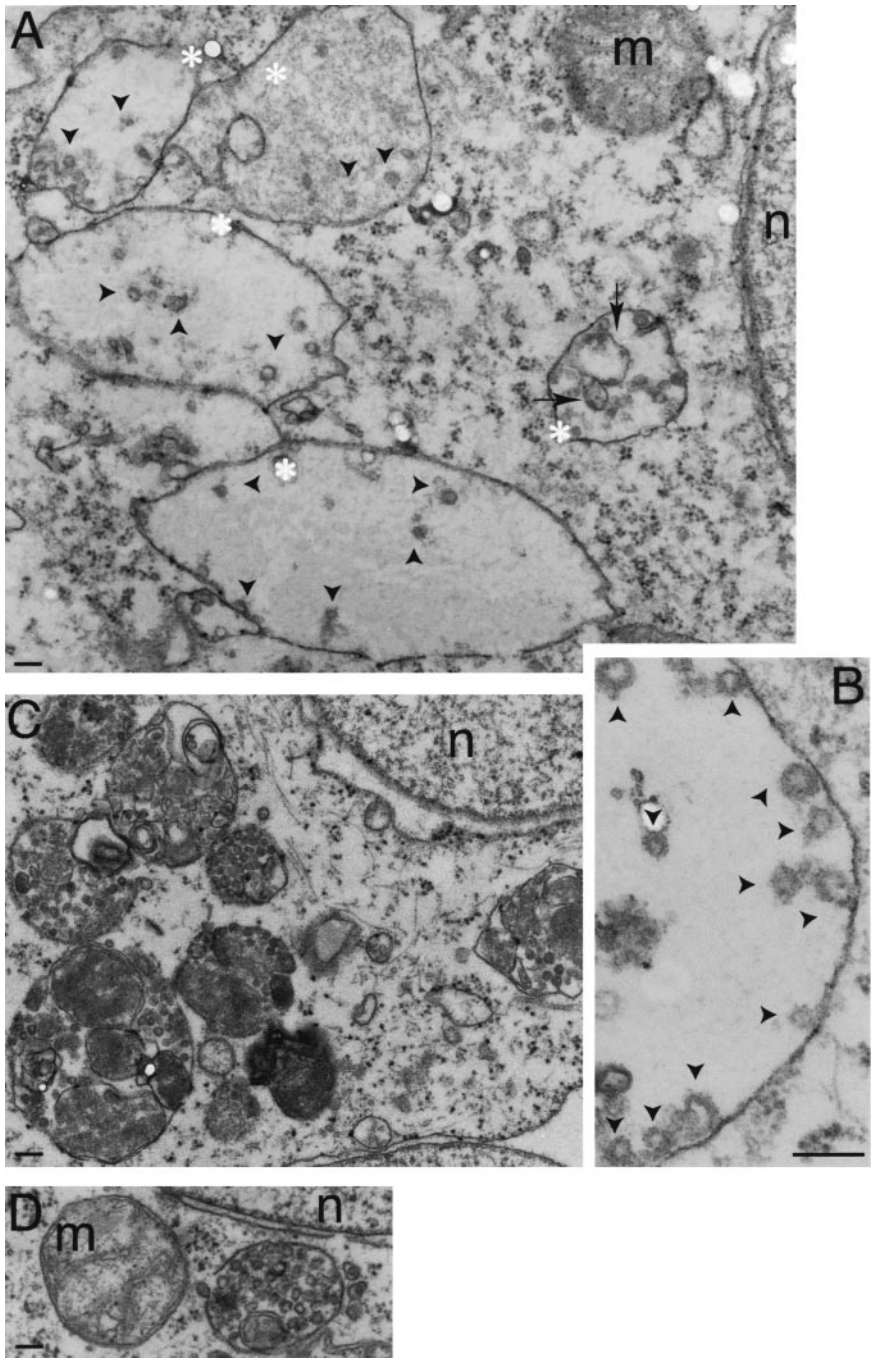

Figure 7. PIKfyve^{K1831E} expression induces formation of enlarged MVB-like structures with reduced number of internal vesicles and membrane whorls. Doxycycline-treated PIKfyve^{K1831E}-expressing (A and B), PIKfyve^{WT}-expressing (C), or parental HEK293 cell lines (D) were observed by electron microscopy as described under MATERIALS AND METHODS. Enlarged MVB-like compartments (asterisks) with relatively fewer lumenal vesicles (arrowheads) and membrane whorls (arrows) are seen in PIKfyve^{K1831E}-transfected cells (A and B). Depicted are the lumenal vesicles relatively to MVB limiting membrane at higher magnification (B). Micrographs are representative of >100 cells observed in two independent experiments. n, nucleus; m, mitochondria. Bar, 0.1 μm.

mechanisms have been proposed to explain the observed defect: a failure of MVBs to inwardly vesiculate and store lumenal vesicles (Fernandez-Borja *et al*., 1999), a failure to recycle membranes to other cellular destinations (Bright *et al*., 2001), or both (Futter *et al*., 2001). Combined data presented here and in our previous studies provide compelling experimental evidence that the key effector in the formation of enlarged MVBs is disrupted PIKfyve function and decreased PtdIns 3,5-P_2 production. Thus, dominant-negative kinase-deficient PIKfyve point mutants induce massive endomembrane vacuolation that could be rescued upon overproduction of PIKfyve^{WT} (Ikonomov *et al*., 2001). In contrast, inhibitory antibodies against hVPS34 dilate MVBs only occasionally (Futter *et al*., 2001). Next, microinjected PtdIns 3,5-P_2 but not PtdIns 3-P, corrects the endomembrane defects induced by the dominant-negative lipid kinase-deficient mutants (Ikonomov *et al*., 2002a). Ultrastructural analysis defines the vacuolated compartments formed due to PIKfyve^{K1831E} expression as MVB-like structures with a reduced number of lumenal vesicles and membrane whorls (Figure 7). Furthermore, through generating PtdIns 3,5-P_2, PIKfyve^{WT} typically decreases PtdIns 3-P levels, yet it has never induced cytoplasmic vacuoles (Ikonomov *et al*., 2001; Figure 2). Finally, in yeast the loss of Fab1p function also results in a formation of grossly enlarged vacuoles and defects in MVB formation (Yamamoto *et al*., 1995; Gary *et al*.,

1998; Odorizzi *et al*., 1998). In fact, published data related to wortmannin-dependent formation of swollen endosomes (Fernandez-Borja *et al*., 1999; Bright *et al*., 2001; Futter *et al*., 2001) could be solely explained by the drug's numerous effects on PIKfyve: 1) elimination of the FYVE finger-directed PIKfyve attachment to key late endosomal membranes due to reduced PtdIns 3-P (200 nM of wortmannin releases inner membrane-bound PIKfyve almost completely; Sbrissa *et al*., 2002a); 2, substrate deprivation by inhibiting PI 3-Ks and PtdIns 3-P production; and 3, direct inhibition of PIKfyve enzymatic activity (ID_{50} = 600 nM; Sbrissa *et al*., 1999). Together, these data define the PIKfyve enzymatic activity and PtdIns 3,5-P_2 production as key regulators in late endosome/MVB morphogenesis.

Recent studies in yeast have identified a set of genes, the class E *VPS*, whose products, assembled in complexes called ESCRT-I, -II, and -III, execute the selection of ubiquitinated membrane proteins into the MVB pathway. These complexes are thought to perform a cascade of events, the last step of which is an ATP-dependent hydrolysis by a AAA-type ATPase, Vps4, to dissociate the ESCRT-III complex, thereby releasing proteins for further rounds of protein sorting (Katzmann *et al*., 2002). Although the function of Fab1p in this process, as well as the operation of a similar mechanism in mammalian MVB sorting is largely unknown, recent data document a functional relationship between SKD1, the mammalian Vps4 ortholog, and PIKfyve (Ikonomov *et al*., 2002b). The SKD1 ATPase activity seems important for the organization of COS cell endocytic membranes defined by PIKfyve, thus placing PIKfyve action downstream of SKD1 (Ikonomov *et al*., 2002b). Based on these and other results and considerations, we propose that PIKfyve activity and PtdIns 3,5-P_2 are necessary at a step(s) after the selection of cargo molecules destined for MVB internal membranes. This may involve the ability of MVB to form and store lumenal vesicles or membrane whorls and/or to export membranes to other compartments for reuse. Further insights into this issue should be forthcoming as we learn more about the potential PtdIns 3,5-P_2-regulated downstream effectors.

Role of PIKfyve and MVB Morphogenesis in the Functioning of Membrane-trafficking Pathways

Endocytosis is typically divided into early events that include budding and internalization of vesicles from the cell surface, in some cases resulting in a return (or recycling) of endocytosed materials to the plasma membrane, and later events that involve transport of internalized material through the membranes of the endosomal system to the lysosomes. Data in this study clearly indicate that PIKfyve is excluded from the mechanism(s) that control the early endocytic events and endosome recycling. This was evidenced here by unaltered rates of both ^{125}I-Tf recycling and HRP uptake at early stages in the presence of overexpressed active or inactive PIKfyve (Figures 3 and 4). These results corroborate our previous findings that intracellular membrane-associated PIKfyve is excluded from the endosomes that recycle Tf or other proteins (Shisheva *et al*., 2001). However, it was indeed surprising that a normal rate of internalization and recycling could be reached in the presence of a massive PIKfyve^{K1831E}-induced formation of swollen endocytic membranes (Figures 2 and 7A). Unlike the early endocytic uptake and the receptor recycling, the fluid phase traffic through the degradative arm of the endocytic pathway was substantially retarded as defined here by the reduced rate of HRP uptake at longer incubation times in PIKfyve^{K1831E}-expressing cells (Figure 3). In contrast to fluid phase endocytosis, the traffic through the degradation pathway of EGFR was not significantly affected by PIKfyve^{K1831E} expression as evidenced here by the normal rate of EGFR degradation (Figure 5). Consistent with these results, the delivery of EGF or EGFR to lysosomes through the endocytic pathway was found to be also unchanged or only slightly inhibited in cells that formed enlarged endocytic structures due to wortmannin (Futter *et al*., 2001). Likewise, the targeting of newly synthesized lysosomal enzymes, exemplified in this study by procathepsin D processing in the lysosomal pathway was not affected by the formation of enlarged MVB-like structures due to PIKfyve^{K1831E} expression (Figure 1B). Together, these results indicate that the requirement for PIKfyve function and PtdIns 3,5-P_2 production is strictly confined to the later stages of the fluid phase endocytic pathway, most likely at MVBs to regulate the internal vesicle formation and lumenal membrane storage as discussed above. This implies that in the presence of enlarged MVBs with reduced internal membranes, endocytosed receptors or biosynthetic protein cargo are delivered to lysosomes likely via the MVB limiting membrane. The fluid phase markers may follow different mechanisms involving late micropinocytic endosomes, shown to be distinct from MPR-positive late endosomes (Hewlett *et al*., 1994; Shurety *et al*., 1998). Consistent with these published data, we also observed somewhat distinct appearances of the late endocytic structures detected by TxR-dextran versus MPR in PIKfyve^{K1831E}-expressing cells (Figure 6). These distinct mechanisms for delivery from late endosomes to lysosomes may explain at least in part the observed defect in the lysosomal pathway of the fluid phase transport but not that of EGFR or the newly synthesized procathepsin D in the presence of expressed PIKfyve^{K1831E}. However, the fact that endocytosed fluid phase markers could reach end lysosomes after an extended incubation time (Figure 6) implies that the formation of MVB-like enlarged structures does not absolutely inhibit MVB-lysosome fusion but rather imposes a kinetic block.

In conclusion, the results presented here indicate that PIKfyve directs synthesis of a specific endosomal pool of PtdIns 3,5-P_2 that is required for MVB inward vesiculation and/or storage of internal vesicles. Defects in this process coincide with a delay in sorting and traffic of peripheral endosomes containing lysosomaly directed fluid phase markers, but do not affect receptor recycling and degradation or protein sorting in the biosynthetic pathway.

ACKNOWLEDGMENTS

We thank Linda McCraw for the excellent secretarial assistance and G. Porcheron-Berthet for technical assistance. We thank Drs. Ellen Tisdale, Bernard Hofflack, Gregory Conner, Aliza Torbati, Ian Trowbridge, and Sue White for the kind gifts of antibodies. This work was supported by National Institute of Health grant DK-58058, American Diabetes Association Research grant (to A.S), and the Fonds National Suisse pour la Recherche Scientifique grants 31-55170.98 and 31-53686.98 (to J.-L.C).

REFERENCES

Bright, N.A., Lindsay, M.R., Stewart, A., and Luzio, J.P. (2001). The relationship between lumenal and limiting membranes in swollen late endocytic compartments formed after wortmannin treatment or sucrose accumulation. Traffic *2*, 631–642.

Brown, W.J., DeWald, D.B., Emr, S.D., Plutner, H., and Balch, W.E. (1995). Role for phosphatidylinositol 3-kinase in the sorting and transport of newly synthesized lysosomal enzymes in mammalian cells. J. Cell Biol. *130*, 781–796.

Carpentier, J.L., Gorden, P., Amherdt, M., Van Obberghen, E., Kahn, C.R., and Orci, L. (1978). 125I-insulin binding to cultured human lymphocytes. Initial

localization and fate of hormone determined by quantitative electron microscopic autoradiography. J. Clin. Investig. *61*, 1056–1070.

Corvera, S. (2001). Phosphatidylinositol 3-kinase and the control of endosome dynamics: new players defined by structural motifs. Traffic *2*, 859–866.

Davidson, H.W. (1995). Wortmannin causes mistargeting of procathespin D. Evidence for the involvement of a phosphatidylinositol 3-kinase in vesicular transport to lysosomes. J. Cell Biol. *130*, 797–805.

Fernandez-Borja, M., Wubbolts, R., Calafat, J., Janssen, H., Divecha, N., Dusseljee, S., and Neefjes, J. (1999). Multivesicular body morphogenesis requires phosphatidylinositol 3-kinase activity. Curr. Biol. *9*, 55–58.

Fruman, D.A., Meyers, R.E., and Cantley, L.C. (1998). Phosphoinositide kinases. Annu. Rev. Biochem. *67*, 481–507.

Futter, C.E., Collinson, L.M., Backer, J.M., and Hopkins, C.R. (2001). Human VPS34 is required for internal vesicle formation within multivesicular endosomes. J. Cell Biol. *155*, 1251–1263.

Gary, J.D., Wurmser, A.E., Bonangelino, C.J., Weisman, L.S., and Emr, S.D. (1998). Fab1p is essential for PtdIns(3)P 5-kinase activity and the maintenance of vacuolar size and membrane homeostasis. J. Cell Biol. *143*, 65–79.

Ghosh, P., Dahms, N.M., and Kornfeld, S. (2003). Mannose 6-phosphate receptors: new twists in the tail. Nat. Rev. Mol. Cell. Biol. *4*, 202–213.

Gillooly, D.J., Morrow, I.C., Lindsay, M., Gould, R., Bryant, N.J., Gaullier, J.-M., Parton, R.G., and Stenmark, H. (2000). Localization of phosphatidylinositol 3-phosphate in yeast and mammalian cells. EMBO J. *19*, 4577–4588.

Griffiths, G., Matteoni, R., Back, R., and Hoflack, B. (1990). Characterization of the cation-independent mannose 6-phosphate receptor-enriched prelysosomal compartment in NRK cells. J. Cell Sci. *95*, 441–461.

Gruenberg, J. (2001). The endocytic pathway: a mosaic of domains. Nat. Rev. Mol. Cell. Biol. *2*, 721–730.

Hewlett, L.J., Prescott, A.R., and Watts, C. (1994). The coated pit and macropinocytic pathways serve distinct endosome populations. J. Cell Biol. *124*, 689–703.

Hopkins, C.R., Gibson, A., Shipman, M., Strickland, D.K., and Trowbridge, I.S. (1994). In migrating fibroblasts, recycling receptors are concentrated in narrow tubules in the pericentriolar area, and then routed to the plasma membrane of the leading lamella. J. Cell Biol. *125*, 1265–1274.

Hunziker, W., and Geuze, H.J. (1996). Intracellular trafficking of lysosomal membrane proteins. Bioessays *18*, 379–389.

Ikonomov, O.C., Sbrissa, D., Mlak, M., Kanzaki, M., Pessin, J., and Shisheva, A. (2002a). Functional dissection of lipid and protein kinase signals of PIKfyve reveals the role of PtdIns 3, 5-P_2 production for endomembrane integrity. J. Biol. Chem. *277*, 9206–9211.

Ikonomov, O.C., Sbrissa, D., and Shisheva, A. (2001). Mammalian cell morphology and endocytic membrane homeostasis require enzymatically active phosphoinositide 5-kinase PIKfyve. J. Biol. Chem. *276*, 26141–26147.

Ikonomov, O.C., Sbrissa, D., Yoshimori, T., Cover, T.L., and Shisheva, A. (2002b). PIKfyve kinase and SKD1 AAA ATPase define distinct endocytic compartments. J. Biol. Chem. *277*, 46785–46790.

Katzmann, D.J., Odorizzi, G., and Emr, S.D. (2002). Receptor downregulation and multivesicular-body sorting. Nat. Rev. Mol. Cell. Biol. *3*, 893–905.

Kundra, R., and Kornfeld, S. (1998). Wortmannin retards the movement of the mannose 6-phosphate/insulin-like growth factor II receptor and its ligand out of endosomes. J. Biol. Chem. *273*, 3845–3853.

Martin, T.F.J. (2001). PI(4, 5)P_2 regulation of surface membrane traffic. Curr. Opin. Cell. Biol. *13*, 493–499.

Martys, J.L., Wjasow, C., Gangi, D.M., Kielian, M.C., McGraw, T.E., and Backer, J.M. (1996). Wortmannin-sensitive trafficking pathways in Chinese hamster ovary cells. J. Biol. Chem. *271*, 10953–10962.

Mayor, S., Presley, J.F., and Maxfield, R.R. (1993). Sorting of membrane components from endosomes and subsequent recycling to the cell surface occurs by a bulk flow process. J. Cell Biol. *121*, 1257–1269.

Miaczynska, M., and Zerial, M. (2002). Mosaic organization of the endocytic pathway. Exp. Cell Res. *272*, 8–14.

Mills, I.G., Jones, A.T., and Clague, M.J. (1999). Regulation of endosome fusion. Mol. Memb. Biol. *16*, 73–79.

Mukherjee, S., and Maxfield, F.R. (2000). Role of membrane organization and membrane domains in endocytic lipid trafficking. Traffic *1*, 203–211.

Nordeng, T.W., Gregers, T.F., Kongsvik, T.L., Méresse, S., Gorvel, J.-P., Jourdan, F., Motta, A., and Bakke, O. (2002). The cytoplasmic tail of invariant chain regulates endosome fusion and morphology. Mol. Biol. Cell *13*, 1846–1856.

Odorizzi, G., Babst, M., and Emr, S.D. (1998). Fab1p PtdIns(3)P 5-kinase function essential for protein sorting in the multivesicular body. Cell *95*, 847–858.

Odorizzi, G., Babst, M., and Emr, S.D. (2000). Phosphoinositide signaling and the regulation of membrane trafficking in yeast. Trends Biochem. Sci. *25*, 229–235.

Pfeffer, S. (2003). Membrane domains in the secretory and endocytic pathways. Cell *112*, 507–517.

Piper, R.C., and Luzio, J.P. (2001). Late endosomes: sorting and partitioning in multivesicular bodies. Traffic *2*, 612–621.

Rijnboutt, S., Stoorvogel, W., Geuze, H.J., and Strous, G.J. (1992). Identification of subcellular compartments involved in the biosynthetic processing of cathepsin D. J. Biol. Chem. *267*, 15665–15672.

Row, P.E., Reaves, B.J., Domin, J., Luzio, J.P., and Davidson, H.W. (2001). Overexpression of a rat kinase-deficient phosphoinositide 3-kinase, Vps34p, inhibits cathepsin D maturation. Biochem. J. *353*, 655–661.

Sbrissa, D., Ikonomov, O., and Shisheva, A. (2001). Selective insulin-induced activation of class I_A phosphoinositide 3-kinase in PIKfyve immune complexes from 3T3–L1 adipocytes. Mol. Cell. Endocrinol. *181*, 35–46.

Sbrissa, D., Ikonomov, O.C., and Shisheva, A. (1999). PIKfyve, a mammalian ortholog of yeast Fablp lipid kinase, synthesizes 5-phosphoinositides. J. Biol. Chem. *274*, 21589–21597.

Sbrissa, D., Ikonomov, O.C., and Shisheva, A. (2002a). PtdIns-3-P interacting domains in PIKfyve: binding specificity and role in PIKfyve endomembrane localizations. J. Biol. Chem. *277*, 6073–6079.

Sbrissa, D., Ikonomov, O.C., Deeb, R., and Shisheva, A. (2002b). Phosphatidylinositol 5-phosphate biosynthesis is linked to PIKfyve and is involved in osmotic response pathway in mammalian cells. J. Biol. Chem. *277*, 47276–47284.

Schu, P.V., Takegawa, K., Fry, M.J., Stack, J.H., Waterfield, M.D., and Emr, S.D. (1993). Phosphatidylinositol 3-kinase encoded by yeast *VPS34* gene essential for protein sorting. Science *260*, 88–91.

Shisheva, A. (2001). PIKfyve: the road to PtdIns 5-P and PtdIns 3, 5-P_2. Cell Biol. Int. *25*, 1201–1206.

Shisheva, A., Rusin, B., Ikonomov, O.C., DeMarco, C., and Sbrissa, D. (2001). Localization and insulin-regulated relocation of phosphoinositide 5-kinase PIKfyve in 3T3-Ll adipocytes. J. Biol. Chem. *276*, 11859–11869.

Shisheva, A., Sbrissa, D., and Ikonomov, O. (1999). Cloning, characterization, and expression of a novel Zn^{2+}-binding FYVE finger-containing phosphoinositide kinase in insulin-sensitive cells. Mol. Cell. Biol. *19*, 623–634.

Shpetner, H., Joly, M., Hartley, D., and Corvera, S. (1996). Potential sites of PI-3 kinase function in the endocytic pathway revealed by the PI-3 kinase inhibitor, wortmannin. J. Cell Biol. *132*, 595–605.

Shurety, W., Stewart, N.L., and Stow, J.L. (1998). Fluid phase markers in the basolateral endocytic pathway accumulate in response to the actin assembly-promoting drug jasplakinolide. Mol. Biol. Cell *9*, 957–975.

Siddhanta, U.M., McIlroy, J., Shah, A., Zhang, Y., and Backer, J.M. (1998). Distinct roles for the p110α and hVPS34 phosphatidylinositol 3′-kinases in vesicular trafficking, regulation of the actin cytoskeleton, and mitogenesis. J. Cell Biol. *143*, 1647–1659.

Simonsen, A., Wurmser, A.E., Emr, S.D., and Stenmark, H. (2001). The role of phosphoinositides in membrane transport. Curr. Opin. Cell Biol. *13*, 485–492.

Spiro, D.J., Boll, W., Kirchhausen, T., and Wessling-Resnick, M. (1996). Wortmannin alters the transferrin receptor endocytic pathway *in vivo* and *in vitro*. Mol. Biol. Cell *7*, 355–367.

Wiley, H.S., and Cunningham, D.D. (1982). The endocytic rate constant. J. Biol. Chem. *257*, 4222–4229.

Yamamoto, A., DeWald, D.B., Boronenkov, I.V., Anderson, R.A., Emr, S.D., and Koshland, D. (1995). Novel PI(4)P 5-kinase homologue, Fab1p, essential for normal vacuole function and morphology in yeast. Mol. Biol. Cell *6*, 525–539.